



Electrochemical and Mechanical Behavior of Sn-Zn-x Lead Free Solders

H. F. Abosheisha¹, Ahmed Abdel Nazeer^{2,*}, A.S. Fouda³

¹Physics and Eng. Mathematics Department, Faculty of Engineering, Tanta University, Tanta 31521, Egypt, E-mail: hatemfouda72@gmail.com

²Electrochemistry and Corrosion Lab., National Research Centre, Dokki, Cairo-12622, Egypt, E-mail:

³Department of Chemistry, Faculty of Science, El-Mansoura University, El- Mansoura-35516, Egypt. Email: asfouda@mans.edu.eg

Received Nov 2011, revised Feb 2012, Accepted 22 Feb 2012-02-21

Corresponding Author: Email: anazeer_nrc@yahoo.com

Abstract

The electrochemical, mechanical, structural and thermal behavior of lead-free SnZn₉, SnZn₉Bi₂, SnZn₉Bi₂Cu₂, SnZn₉Bi₂Ag₂ solder alloys were investigated by different methods and compared with conventional eutectic tin-lead solder. Results of differential scanning calorimeter (DSC) analysis showed that alloying of Bi to SnZn₉ decreases the melting temperature from 198 °C to 195.9 °C and also the alloying of Cu and Ag to SnZn₉Bi₂ resulted in reducing the melting temperature more to become 194.5 °C and 194 °C, respectively. The addition of different elements to SnZn₉ alloy system such as Ag and Cu allows many complex intermetallic (IMC) phases to form as shown by XRD. The electrochemical behaviour of these alloys in 3.5% NaCl solution was studied using potentiodynamic polarization and electrochemical frequency modulation (EFM) techniques and the results obtained are in good agreement.

Keywords: Lead-free solder alloys, thermal properties, NaCl, potentiodynamic polarization, EFM.

1. Introduction

Tin-lead solders have been widely used in electronics and optoelectronic packaging for a long time, due to their low cost, good soldering properties, low melting temperature, and adequate physical and mechanical properties. However, due to environmental issues, lead is a very toxic metal and its compounds are poisonous. The use of these compounds will not only bring environmental pollution concerns, but also will impair worker's health. The restriction of lead use in industry has been strongly promoted to protect the environment. US EPA (Environmental Protection Agency), Japan and European union tend to forbid the use of lead-containing products [1-3]. The search for lead-free solders with equivalent mechanical properties and microstructural stability to eutectic tin-lead solder is an urgent task. Solder joints are usually exposed to atmospheres that can induce corrosion attack. Corrosion resistance of the solders determines the interconnection life and thus the component life. SnZn₉ is a promising alternative for eutectic Sn-Pb solder due to its low cost and tensile and creep resistance which are better than eutectic Sn-Pb solder. It also exhibit better fatigue life than eutectic Sn-Pb solder [4, 5] and has low melting point (198 °C). The addition of Zn into Sn base alloys has been known to provide mechanical integrity to electronics packaging [6]. Also, the small addition of Bi will be advantageous to improve the soldering property in electronic packaging by lowering melting temperature than the eutectic Sn-Zn solder alone. Therefore, the addition of some Bi element will have good effect on the mechanical properties of SnZn₉ [7, 8]. However, alloys with high Bi concentration need to be controlled because of the brittle nature of Bi and the strong tendency for segregation

[9, 10]. The aim of this study is to assess the electrochemical, mechanical and electrical behavior of lead-free SnZn₉, SnZn₉Bi₂, SnZn₉Bi₂Cu₂ and SnZn₉Bi₂Ag₂ solder alloys in 3.5% NaCl solution.

2. Experimental

Tin, Zinc, Bismuth, Silver, Copper 99.99 mass% purity, were prepared by a liquid metallurgy route. The alloys melt were solidified in cast-iron mould in the form of 100mm × 15mm × 10mm. All the electrochemical measurements were performed using a potentiostat/galvanostat (Gamry PCI 300/4). A three-electrode cell of Pyrex glass, consisting of a saturated calomel electrode (SCE) as a reference electrode, a platinum foil as counter electrode, and the alloy specimen as a working electrode is used. This was machined into test electrodes of dimensions 1 x 1 cm² and fixed in polytetrafluoroethylene (PTFE) rods by epoxy resin in such a way that only one surface; of area 1cm² was left uncovered. The exposed surface was wet-polished with silicon carbide abrasive paper (up to 1200 grit), degreased in acetone, rinsed with doubly distilled water, and then dried by dry air. All measurements were carried out in aerated solution of 3.5% NaCl. The potentiodynamic polarization measurements were performed at potentials in the range from -1700 mV_{SCE} to -400 mV_{SCE} at a scan rate of 1 mVs⁻¹.

The electrochemical frequency modulation data have been analyzed using Echem analyst 5.21. In this work, potential perturbation signal with amplitude of 10 mV with two sine waves of 2 and 5 Hz was applied. The intermodulation spectra contain current responses assigned for harmonical and intermodulation current peaks. The larger peaks were used to calculate the corrosion current density (*i*_{corr}), the Tafel slopes (β_a and β_c) and the causality factors CF2 and CF3.

X-Ray diffraction analysis was performed on the flat surface of all alloys using an X-ray diffractometer (Dx-30, Shimadzu, Japan) of Cu-K _{α} radiation and Ni-filter in the range from 20° to 100° of 2 θ value (λ = 0.154056 nm, 4.5kV and 35mA). Phase identification was carried out by matching each characteristic peak with the data cards. Bulk hardness of all the alloys was measured using a digital Vickers hardness tester, under a load of 1 KN. The application time of the load was 20 seconds. Melting temperature has been measured by differential thermal analysis (DTA) with heating rate 10 K/min. All samples have the same mass (0.2 mg).

3 Results and Discussion

3.1 X-Ray diffraction study

X-ray diffraction method was used to determine the phases of the five solder alloys, see Fig. 1 (a-e). The pattern in Fig. (1a) indicates the formation of both phases of Sn and Pb. However, Fig. 1 (b-e) shows that Sn and Zn phases are the main constituents. From Fig. 1 (c-e), it is clear that Bi is absent which means a complete solubility of Bi in Sn matrix [11]. The addition of 2 wt. % Ag or Cu leads to the formation of the intermetallic compounds SnAg₃ and Sn₅Cu₆, respectively, as can be deduced from Fig. 1(d, e). These results are consistent with that of Chang et al [12].

3.2 Melting temperature

Melting temperature is a critical solder characteristic because it determines the maximum operating temperature of the system and the minimum processing temperature its components must survive [13]. DSC analysis was carried out in order to investigate the fundamental thermal reactions on heating of the solder alloy. Fig. 2 shows the thermographs (relation between heat flow (μ V) and temperature (°C)) of the used alloys. Table 1 shows the melting temperatures of the investigated SnZn₉, SnZn₉Bi₂, SnZn₉Bi₂Cu₂ and SnZn₉Bi₂Ag₂ alloys. With the addition of Bi element, the melting temperatures decreased slightly where the melting temperature was 195.9 °C as compared to 198 °C for SnZn₉ eutectic alloy which improve the soldering properties in electronic packaging [14]. The addition of an amount of 2 wt.% of Cu and Ag lowers the melting temperature of the solder significantly. It decreases from 198 °C for SnZn₉ to 194.5 and 194 °C for the SnZn₉Bi₂Cu₂ and SnZn₉Bi₂Ag₂ alloys respectively.

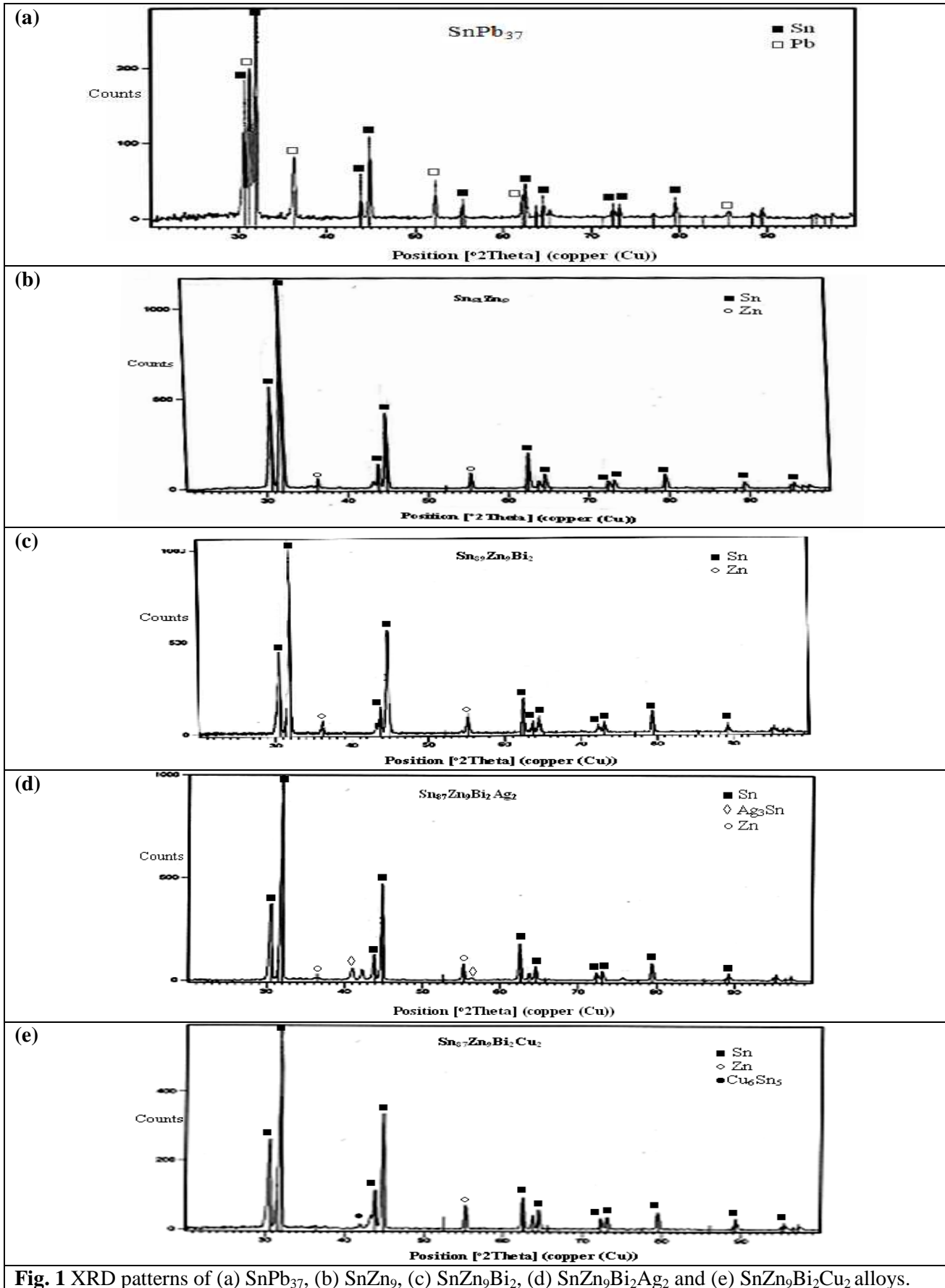


Fig. 1 XRD patterns of (a) SnPb_{37} , (b) SnZn_9 , (c) SnZn_9Bi_2 , (d) $\text{SnZn}_9\text{Bi}_2\text{Ag}_2$ and (e) $\text{SnZn}_9\text{Bi}_2\text{Cu}_2$ alloys.

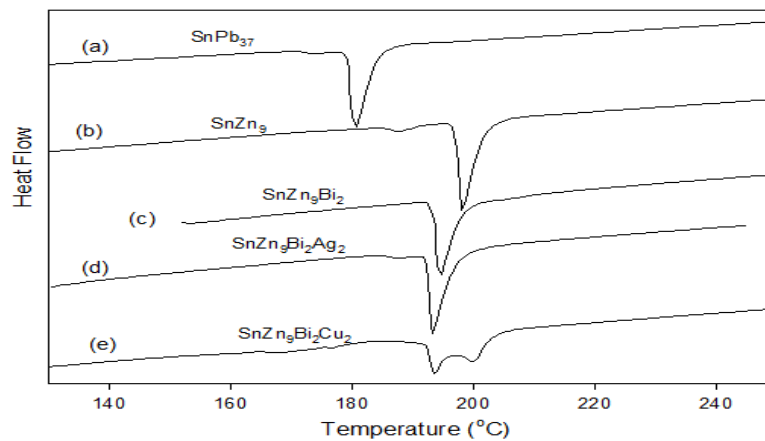


Fig. 2 DSC curves of (a) SnPb₃₇, (b) SnZn₉, (c) SnZn₉Bi₂, (d) SnZn₉Bi₂Ag₂ and (e) SnZn₉Bi₂Cu₂ solder alloys.

Table 1. Melting temperature of the tested alloys

Alloy	Melting Temperature (°C)
SnPb ₃₇	182.1
SnZn ₉	198
SnZn ₉ Bi ₂	195.9
SnZn ₉ Bi ₂ Cu ₂	194.5
SnZn ₉ Bi ₂ Ag ₂	194

3.3 Hardness

The results of the bulk Vickers hardness measurements are given in Table 2. It was noticed that it is 253 MPa for SnZn₉Bi₂ while in case of SnZn₉Bi₂Ag₂ and SnZn₉Bi₂Cu₂ the values were increased to 275 and 383.9 MPa, respectively. The observed increase in the values of hardness by adding Cu or Ag to ternary SnZn₉Bi₂ alloy due to presence of hard intermetallic compound, which act as hard inclusions in the soft matrix.

Table 2. Vickers hardness of the tested alloys

Alloy	Vickers Hardness (MPa)
SnPb ₃₇	126
SnZn ₉	254.9
SnZn ₉ Bi ₂	253
SnZn ₉ Bi ₂ Cu ₂	383.9
SnZn ₉ Bi ₂ Ag ₂	275

3.4 Electrochemical tests

3.4.1 Open-circuit potential measurements

Fig. 3(a,b) represents the variation of the open circuit potential (OCP) of lead-free SnZn₉, SnZn₉Bi₂, SnZn₉Bi₂Cu₂, SnZn₉Bi₂Ag₂ solder alloys and SnPb₃₇ alloy for comparison with time for 60 min in 3.5% chloride solution. From Fig. 3a, it is obvious that the steady state potential for SnZn₉ was reached within about 40 min (-989 mV_{SCE}) while for SnZn₉Bi₂, SnZn₉Bi₂Cu₂ and SnZn₉Bi₂Ag₂ alloys, it was reached within the first 20 min from electrode immersion in chloride solution and their values are about -1054, -1046 and -1038 mV_{SCE} respectively. The OCP of all alloys are shifted towards more negative values before it reaches the steady state. Fig. 3b represents the potential time curve for SnPb₃₇ alloy, the steady state potential of the

alloy is reached through the first 20 min from electrode immersion in chloride solution. The OCP of the alloy shifts towards more negative values during the period of the measurement until reach the steady state and its value is about -491 mV.

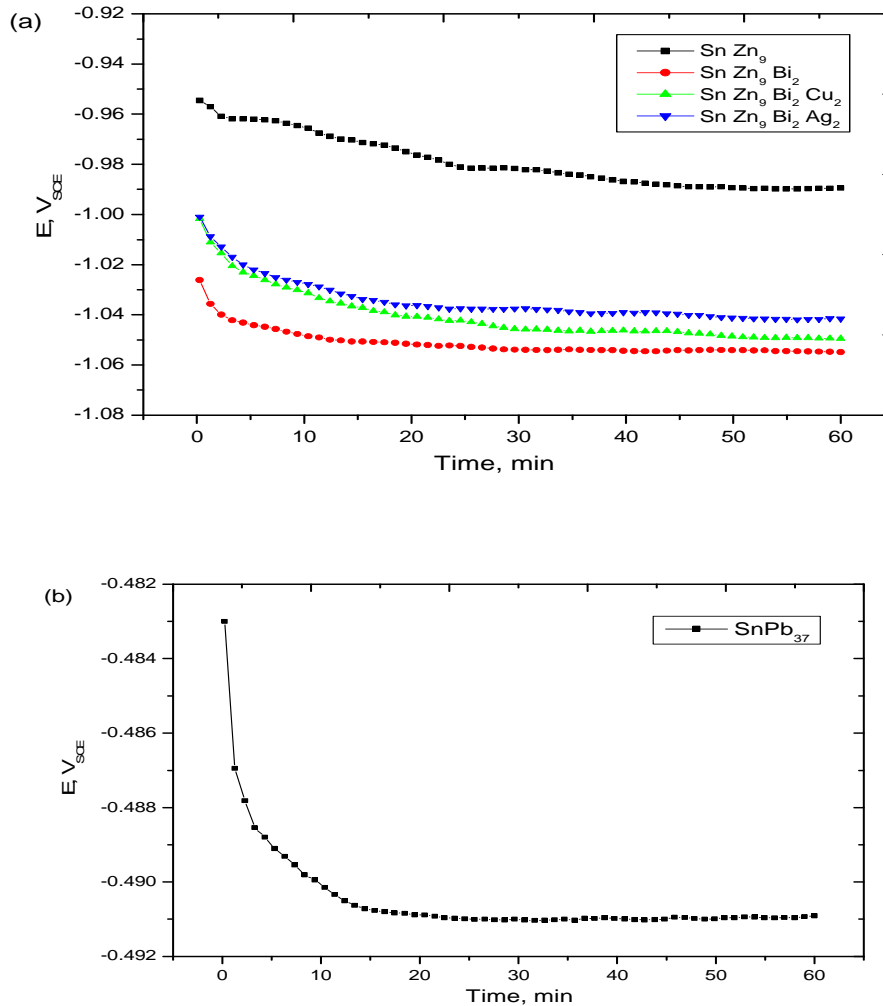


Fig. 3 Potential-time plots for (a) lead-free SnZn₉, SnZn₉Bi₂, SnZn₉Bi₂Cu₂ and SnZn₉Bi₂Ag₂ solder alloys and (b) SnPb₃₇ alloy in 3.5% NaCl solution.

3.4.2 The potentiodynamic polarization curves

The potentiodynamic polarization curves of lead-free SnZn₉, SnZn₉Bi₂, SnZn₉Bi₂Cu₂ and SnZn₉Bi₂Ag₂ solder alloys in 3.5% NaCl solution are shown in Fig. 4. Since all corrosion tests were performed in aerated NaCl solution, the cathodic branch of polarization curves may be ascribed to the dissolved oxygen reduction reaction [15]:



SnZn₉Bi₂Cu₂ solder alloy exhibits the lowest equilibrium potential, -1.336 V_{SCE}, as shown in Table 3 which increases to -1.332 V_{SCE} in case of SnZn₉Bi₂Ag₂, and increases more to -1.325 V_{SCE} in case of SnZn₉ and becomes -1.308 V_{SCE} for SnZn₉Bi₂. On scanning in the anodic direction, the curve of SnZn₉ alloy is characterized by a major anodic peak followed by a gradual active to passive transition. Beyond the peak, a small passive region of about 100 mV_{SCE} is observed followed by a rapid increase in the anodic current indicating the start of pitting attack. The anodic curve of SnZnBi is characterized by a passive region extending for about 150 mV_{SCE}. At the end of the passive region the current increases abruptly as a consequence of the pitting initiation process and hence the passivity breakdown. As previously reported, the

addition of Bi to SnZn₉ solder slightly increases the corrosion resistance in a salt solution [16-18]. For SnZn₉Bi₂Ag₂ and SnZn₉Bi₂Cu₂ alloys there are evidence of a passivation process beginning at about -1.270 V_{SCE} and extending to about -1.070 V_{SCE}, at which passivation disappear when a sharp increase of anodic current density occurs due to the breakdown of the passivation film.

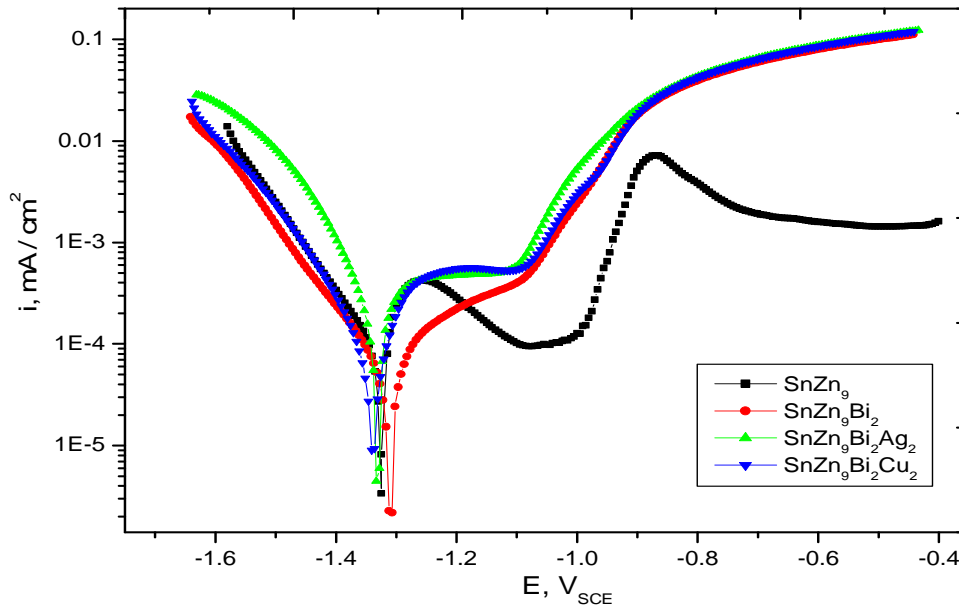


Fig. 4 Potentiodynamic polarization curves of lead-free SnZn₉, SnZn₉Bi₂, SnZn₉Bi₂Cu₂ and SnZn₉Bi₂Ag₂ solder alloys in 3.5% NaCl solution.

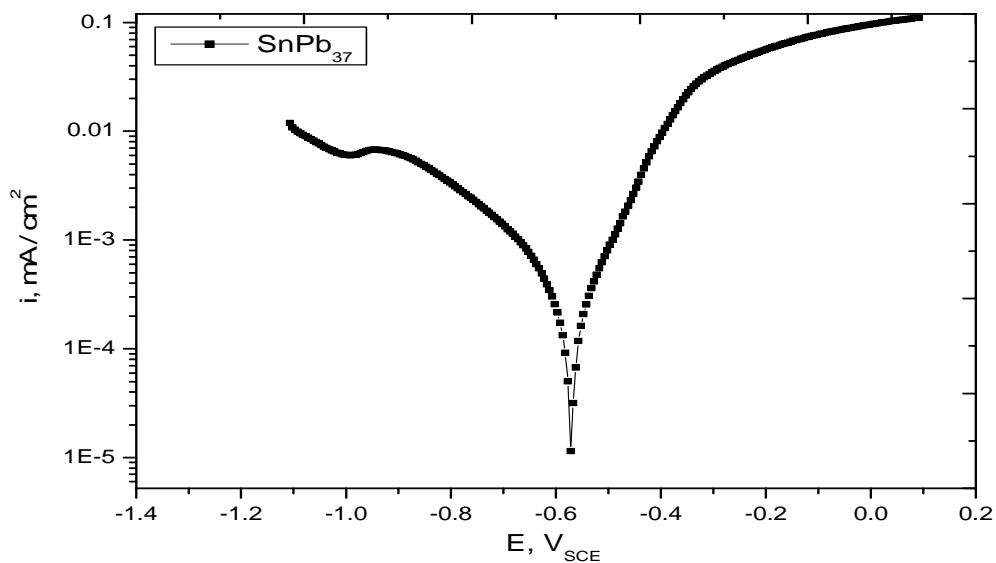


Fig. 5 Potentiodynamic polarization curve of SnPb₃₇ alloy in 3.5% NaCl solution.

Table 3. Electrochemical parameters obtained from potentiodynamic polarization measurements of lead-free SnZn₉, SnZn₉Bi₂, SnZn₉Bi₂Cu₂, SnZn₉Bi₂Ag₂ solder alloys and SnPb₃₇ for comparison in 3.5% NaCl solution

The alloy	i_{corr} , $\mu\text{A cm}^{-2}$	$-E_{corr}$, V	$-\beta_c$, mV decade^{-1}	β_a , mV decade^{-1}	corrosion rate (CR) mm/y
SnPb ₃₇	17.84	0.573	379.5	272.6	37.64
SnZn ₉	69.72	1.325	123.9	174.5	147.11
SnZn ₉ Bi ₂	27.85	1.308	145.5	252.4	58.76
SnZn ₉ Bi ₂ Cu ₂	33.40	1.336	133.7	280.9	70.47
SnZn ₉ Bi ₂ Ag ₂	57.10	1.332	121.9	290.7	120.48

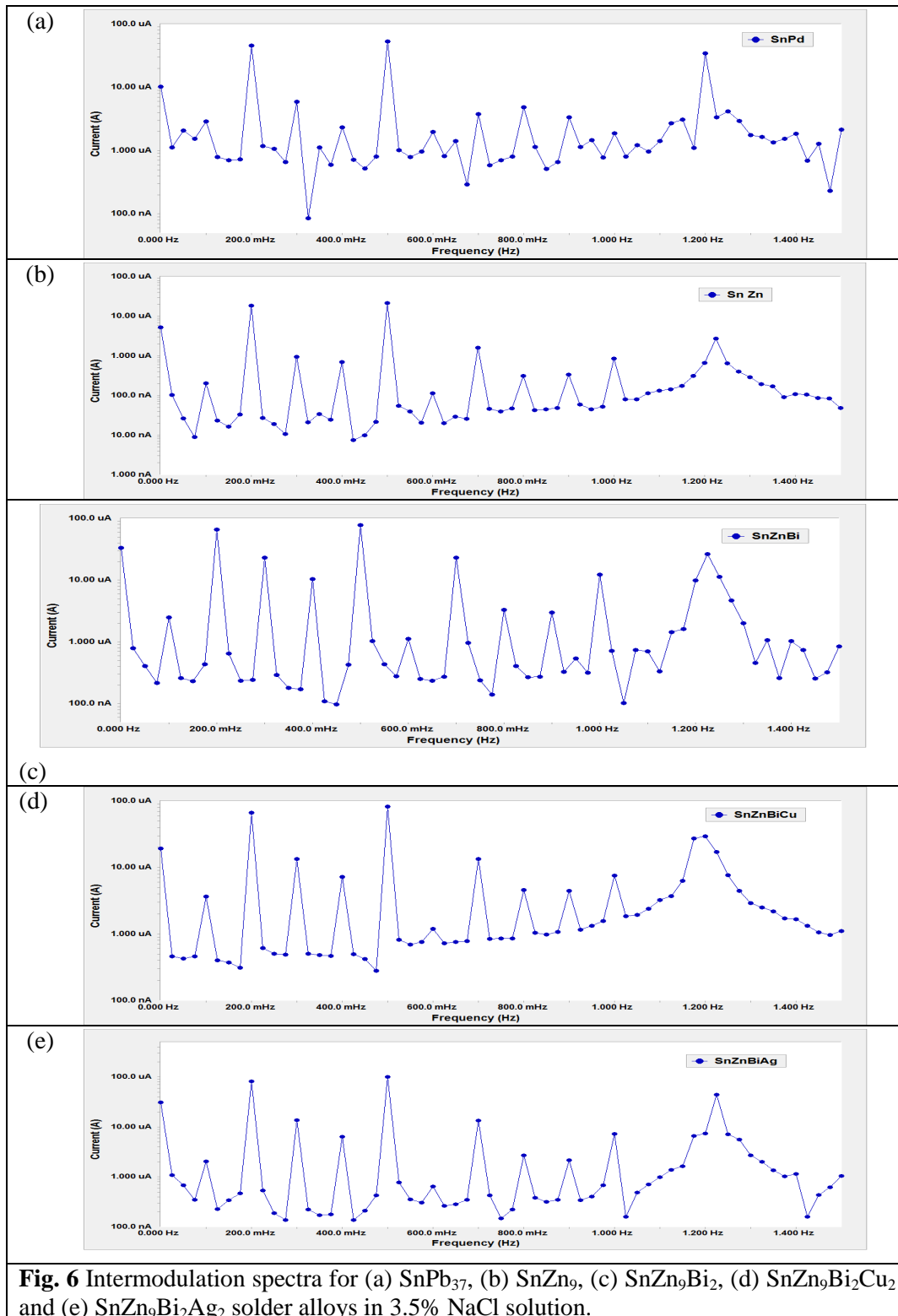
3.4.3 Electrochemical frequency modulation (EFM)

EFM is a non-destructive corrosion measurement technique. In which current responses due to a potential perturbation by one or more sine waves are measured at more frequencies than the frequency of the applied signal, for example at zero harmonic and intermodulation frequencies [19]. The great strength of the EFM is the causality factors which serve as an internal check on the validity of the EFM measurement [20]. The results of EFM experiments are a spectrum of current response as a function of frequency. The spectra contain current responses assigned for harmonical and intermodulation current peaks.

The results of EFM experiments are a spectrum of current response as a function of frequency. The spectrum is called the intermodulation spectrum and examples for behavior of lead-free SnZn₉, SnZn₉Bi₂, SnZn₉Bi₂Cu₂ and SnZn₉Bi₂Ag₂ solder alloys in 3.5% NaCl solution are shown in Fig. 6 (a-e). The larger peaks were used to calculate the corrosion current density (i_{corr}), the Tafel slopes (β_c and β_a) and the causality factors (CF-2 and CF-3). These electrochemical parameters were simultaneously determined and listed in Table 4. As can be seen from this Table, the corrosion current density (i_{corr}) of SnZn₉Bi₂ decreased than in case of SnZn₉ alone from 77.84 $\mu\text{A cm}^{-2}$ for SnZn₉ to 26.90 $\mu\text{A cm}^{-2}$ for SnZn₉Bi₂. In case of SnZn₉Bi₂Cu₂, it is shown that i_{corr} is lower than SnZn₉ but higher than SnZn₉Bi₂ and its value is 36.47 $\mu\text{A cm}^{-2}$. Also for SnZn₉Bi₂Ag₂ alloy, it is obvious that the addition of Ag to SnZn₉Bi₂ increase the value of i_{corr} to 72.04 $\mu\text{A cm}^{-2}$, which is more than that in case of the addition of Cu, i.e. the corrosion resistance of SnZn₉Bi₂ is higher than SnZn₉Bi₂Cu₂ which is higher than SnZn₉Bi₂Ag₂. Also the causality factors CF-2 and CF-3 are close to their theoretical values of 2 and 3, respectively indicating that the measured data are of high quality [21].

Table 4. Electrochemical kinetic parameters obtained by EFM technique for lead-free SnZn₉, SnZn₉Bi₂, SnZn₉Bi₂Cu₂, SnZn₉Bi₂Ag₂ solder alloys and SnPb₃₇ for comparison in 3.5% NaCl solution.

The alloy	i_{corr} , $\mu\text{A cm}^{-2}$	β_a , mV decade^{-1}	β_c , mV decade^{-1}	CF-2	CF-3	CR, mm/y
SnPb ₃₇	18.51	22.56	56.08	2.1	3.11	39.06
SnZn ₉	77.84	41.64	85.3	2.04	2.92	164.24
SnZn ₉ Bi ₂	26.90	74.63	105.5	1.72	2.78	56.76
SnZn ₉ Bi ₂ Cu ₂	36.47	27.21	38.94	1.81	2.88	76.95
SnZn ₉ Bi ₂ Ag ₂	72.04	50.56	93.31	1.97	2.87	152.0



Conclusion

The electrochemical and mechanical behavior of SnZn solders pastes (SnZn₉, SnZn₉Bi₂, SnZn₉Bi₂Cu₂ and SnZn₉Bi₂Ag₂) with SnPb₃₇ solder was studied. The data obtained confirmed that the addition of Bi to SnZn₉ alloy increases its resistance to corrosion also the addition of Cu and Ag to SnZn₉Bi₂ increases the corrosion resistance than SnZn₉ alloy but less than SnZn₉Bi₂. The EFM measurements are in good agreement with the

potentiodynamic. The addition of Bi decreased the melting point of the SnZn₉ solder alloy which decreases more by the addition of Cu and Ag, respectively. The results of the test for Vickers hardness revealed that SnZn₉Bi₂Cu₂ and SnZn₉Bi₂Ag₂ have the highest hardness due the addition of Cu and Ag to SnZn₉Bi₂ alloy.

References

1. US Environmental Protection Agency, Strategy for Reducing Lead Exposure, 21 Feb., 1991.
2. US Environmental Protection Agency, Advanced Notice of Rulemaking, 13 May, 1991.
3. US Environmental Protection Agency, Comprehensive Review of Lead in the Environment under TSCA, 56FR22096-98, 13 May, 1991.
4. Mavoori, H., Chin, J., Vaynman, S., Moran, B., Keer, L., Fine, M. *J. Elec. Mater.*, 26 (7) (1997) 783.
5. Mahmudi, R., Geranmayeh, A. R., Noori, H., Khanbareh H., Jahangiri, N. *Journal of Materials Science: Materials in Electronics*, 20 (4) (2009) 312.
6. Chonan, Y., Komiyama, T., Onuki, J., Urao, R., Kimura, T., Nagano, T. *Materials Transactions* 43 (8) (2002) 1887.
7. Kim, Y.S., Kim, K.S., Hwang, C.H., Sukanuma, K. *Journal of Alloys and Compounds* 352 (2003) 237.
8. Islam, R. A., Chan, Y.C., Jillek, W., Islam, S. *Microelectronics Journal* 37 (2006) 705.
9. Sukanuma, K., Hur, S.H., Kim, K.S., Nakase, H., Nakamura, Y. *Mater. Trans. JIM* 42 (2001) 286.
10. Sengupta, S., Soda, H., McLean, A. *J. Mater. Sci.* 37 (2002) 1747.
11. Islam, M.N., Chan, Y.C., Rizvi, M.J., Jillek, W. *Journal of Alloys and Compounds* 400 (2005) 136.
12. Chang, T.C., Wang, M.C., Hon, M.H. *J. Cryst. Growth* 252 (2003) 391.
13. Glazer, J. *J. Elec. Materi.* 23(8) (1994) 693.
14. Sharif, A., Chan, Y.C. *Microelectron. Eng.* 84 (2) (2007) 328.
15. Mohanty, U.S., Lin, K.L. *J. Electrochem. Soc.* 153 (2006) 319.
16. Aballe, A., Bethencourt, M., Botana, F.J., Cano, M.J., Marcos, M. *Corros. Sci.* 43 (2001) 1657.
17. Boxley, C.J., Watkins, J.J., White, H.S. *Electrochem. Solid-State Lett.* 6 (2003) 38.
18. Liu, C.Y., Chen, Y.R., Li, W.L., Hon M.H., Wang, M.C. *J. Elec. Mater.*, 36 (2007) 11.
19. Kus, E., Mansfeld, F. *Corros. Sci.* 48 (2006) 965.
20. Bethencourt, M., Botana, F.J., Calvino, J.J., Marcos, M. *Corros. Sci.* 40 (1998) 1803.
21. Gamry Echem. Analyst Manual, (2003).

(2012) www.jmaterenvironsci.com